Magnetoelastic stress in Cu/Ni/Cu/Si(100) epitaxial thin films

M. Ciria,* J. I. Arnaudas, and A. del Moral
Departamento de Magnetismo, Departamento de Física de la Materia Condensada and Instituto de Ciencia de Materiales de Aragón, Universidad de Zaragoza and Consejo Superior de Investigaciones Científicas, Zaragoza, Spain

R. C. O'Handley
Department of Materials Science and Engineering, Massachusetts Institute of Technology, Cambridge, Massachusetts, USA
(Received 23 January 2004; published 31 August 2004)

The magnetoelastic (ME) stresses for a series of Cu/Ni(t_{Ni})/Cu/Si(001) epitaxial films are reported. The direct measurement of the stresses in the (001) plane allows determination of the irreducible ME stress $B_{eff}^{\gamma,2}$ that accounts for the breaking of the in-plane square symmetry. $B_{eff}^{\gamma,2}$ has been determined as a function of the applied magnetic field (±15 kOe) and the temperature (300–10 K) for t_{Ni} ranging from 5 to 15 nm. The temperature dependence of $B_{eff}^{\gamma,2}$ is proportional to the square power of the reduced magnetization and the 0 K value increases with the internal stress. These experimental observations are explained considering the tetragonal distortion of the nickel caused by the epitaxial strain that the copper lattice introduces in the nickel layers.

DOI: 10.1103/PhysRevB.70.054431 PACS number(s): 75.70.Ak, 75.80.+q, 75.30.Gw

I. INTRODUCTION

One of the majors achievements obtained by growing epitaxial thin films is the possibility of preparing new structures with controlled composition and properties. Thus, using molecular beam epitaxy, the magnetic impurity concentration in magnetic semiconducting thin films can be selected to exceed the thermodynamical equilibrium concentration value which raises its Curie temperature.[1] Another important achievement is the preparation of single-crystalline thin films with an anisotropic distortion of its crystal lattice.[2] This is possible because epitaxy allows the growing of one element onto another with different lattice parameter. Thus, the cubic symmetry of metals, such as nickel,[3] or oxides, such as $La_{1/3}Ca_{2/3}MnO_3$,[4] undergoes a tetragonal distortion that can be as large as a 2.5% and persists for thickness as large as 200 nm. From a magnetic point of view the relation between distortion and magnetism is a result of the magnetoelastic (ME) inverse effect (or Villari effect) that reflects the influence of the lattice distortion on the spin orientation through the spin-orbit coupling. Thus, the presence of a ME anisotropy energy that overcomes the magnetostatic energy explains, in nickel [5] or manganite thin films,[6] the startling perpendicular magnetic anisotropy (PMA) effect. The surface atoms can also produce PMA as is observed in iron films below 5 atomic layers.[7] More specifically, a lot of work has been done to relate magnetic properties with the strain state in magnetic thin films, because controlling the magnetic anisotropy is important for practical purposes. The key magnetic parameters to understand the relation between lattice deformation and magnetism are the ME coupling coefficients since they indicate the strength of the coupling between the lattice distortion and the magnetic moment structure. Direct measurements of the irreducible ME coefficients has revealed the importance of the strain and surface contributions in 3*d* (Refs. 8–10) and rare-earth [11] metals. In the latter systems the ME stresses, measured a function of temperature, have revealed surface and volume contributions in the framework of the single-ion theory.[11] Thus, extending the measurement of the ME stress to low temperature in 3*d* systems can contribute to the understanding of the physical origin of the contributions to the ME anisotropy energy density. In this work we present direct measurements of the thermal dependence of the irreducible ME stress coefficient $B_{eff}^{\gamma,2}$ responsible for the breaking of the in-plane cubic symmetry in a series of epitaxial Cu/Ni(t_{Ni})/Cu/Si(001) films, with t_{Ni} ranging from 5 to 15 nm. This system is interesting because at room temperature, the Ni undergoes a spin reorientation from out-of-plane to in-plane magnetization at $t_{Ni} \simeq 12$ nm and the Ni films are in a state of large anisotropic strain.[3] This fact produces a large ME contribution to the anisotropy energy that is very important in thin films because the magnetocrystalline anisotropy energy in nickel has a small value. In the (001) plane, the latter contribution although small favors the [110] as the easy direction.

From the thermal dependence of the irreducible ME stress and the thickness dependence of $B_{eff}^{\gamma,2}$ at 0 K, we observe, first, that $B_{eff}^{\gamma,2}(T=0)$ is larger than the value obtained for a 200 nm thick film and tends to increase as t_{Ni} decreases and, secondly, that the thermal dependence of $B_{eff}^{\gamma,2}$, studied as a function of powers of the reduced magnetization m is fitted with the same exponent 2 that applies to the bulk material. These results are discussed in terms of a volumelike contribution to the ME energy density.

II. EXPERIMENT

The films studied in this work have been prepared by *e*-beam evaporation in a UHV chamber. The Cu(nm)/Ni(t_{Ni})/Cu(200 nm) structure was grown onto Si(001) wafers. Details of the growing procedure can be found elsewhere.[3] The ME stress was measured by a cantilever beam technique. The technique is described in Ref. 15. The length of cantilever beam is about 1 cm. For all the

samples, the width-to-length ratio of the cantilever was kept at 0.5. The cantilever is cut along the Ni [100] crystallographic direction, which is the [110] direction of the Si wafer. The breaking of the in-plane square symmetry, defined by the irreducible stress coefficient $B_{\mathrm{eff}}^{\gamma,2}$ is obtained by measuring the stress along the [100] direction, while the magnetic field is applied, ranging from +15 to −15 kOe, longitudinally σ_l and transversally σ_t to the cantilever beam direction. The evaluation of $\sigma_l - \sigma_t$, that is, $B_{\mathrm{eff}}^{\gamma,2}$, can be related to measurable quantities

$$B_{\mathrm{eff}}^{\gamma,2} = \sigma_l - \sigma_t = \frac{1}{3}\frac{E}{1+\nu}\frac{t_s^2}{t_f}\frac{1}{L^2}(\Delta_l - \Delta_t), \qquad (1)$$

where the ME stress and beam deflection Δ are related by the modified Stoney equation,[12] E and ν are the Young's modulus and Poisson ratio of the silicon, t_s and t_f are the silicon and magnetic thin film thicknesses and L is the beam length. The Si elastic constants vary less than 2% from 77 K to 290 K,[13] for this reason we have taken an average value for E and ν for all the range of temperatures. Due to small number of nickel layers in the system, to increase the sensitivity of the technique the wafer thickness was thinned down to about 200 μm.

The domain structure of the Cu/Ni(t_{Ni})/Cu/Si(001) films was studied at room temperature, in air, by means of a magnetic force microscope. The magnetic tips used were obtained by sputtering about 30 nm of cobalt on commercial Si cantilevers.

III. RESULTS

A. Magnetoelastic stress isotherms

Figure 1 shows selected ME stress isotherms for Cu/Ni/Cu/Si(001) thin films at various temperatures. Each panel includes both σ_l and σ_t curves, for each temperature and t_{Ni} selected. The temperature ranges from 20 to 280 K, and measurements for t_{Ni}=5, 8, 12, and 15 nm are displayed. The arrow in Fig. 1(a) indicates the difference $\sigma_l - \sigma_t$ that corresponds to $B_{\mathrm{eff}}^{\gamma,2}$. The measurements show that on increasing temperature the field needed to saturate the films decreases. This fact is illustrated in Figs. 1(a)–1(d), where the 280 and 20 K curves, for t_{Ni}=15 nm, and the 250 and 80 K isotherms, for t_{Ni}=12 nm are displayed. The measurements performed at 250 and 280 K are saturated at 5 kOe while the 20 and 80 K isotherms need magnetic fields as large as 15 KOe. This fact indicates that the perpendicular effective magnetic anisotropy increases its value with decreasing temperature, with respect to the room temperature value.

Other interesting facts include the σ_t stress: (a) the small values for the σ_t isotherms compared with the values obtained for σ_l and (b) the change in sign of σ_t, measured as the difference between the ME stress at the saturation and the coercive field, from positive to negative values, as t_{Ni} increases. This fact is more clearly observed in Fig. 2 that shows σ_t for t_{Ni}=5, 8, 12, and 15 nm at 100 K.

B. Magnetic force microscopy images

The domain images obtained for the Ni epitaxial films are shown in Fig. 3. The images show clear differences between films with thicknesses below and above 10 nm. For the 6 and 8 nm thick films [Figs. 3(a) and 3(b), respectively], the images show a structure formed by large domains, with strong contrast between the up and down domains. For both films the domains are very large although the length of the domain wall surrounding a given domain is clearly larger in the 8nm thick film that shows how the wall turns one way and another

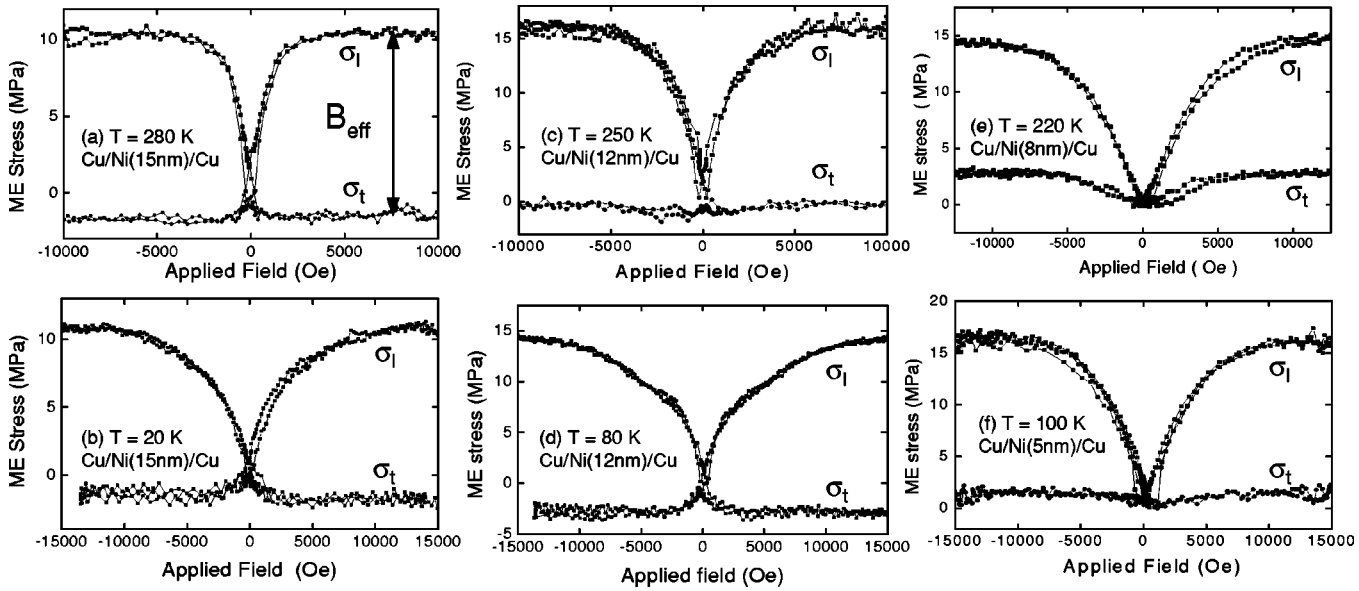

FIG. 1. Magnetoelastic stress curves for a Cu/Ni/Cu/Si(001) films as a function of temperature (a) 280 K, (b) 20 K, (c) 250 K, (d) 80 K, (e) 220 K, (f) 100 K, and the film thickness: (a), (c) 15 nm, (b), (d) 12 nm, (e) 8 nm, and (f) 5 nm. The applied magnetic field was applied along the [100] σ_l and [010] σ_t crystallographic directions. The cantilever beam is cut along the nickel [100] crystallographic direction.

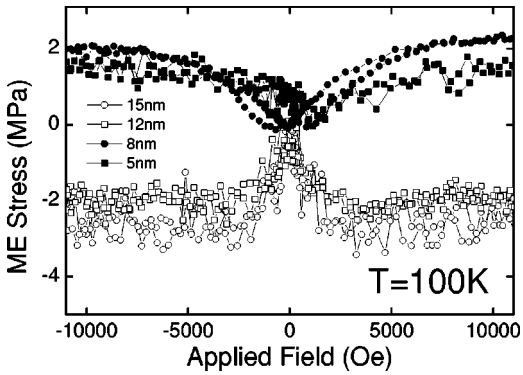

FIG. 2. ME transversal stress isotherms σ_t for $t_{Ni}=5$, 8, 12, and 15 nm at 100 K.

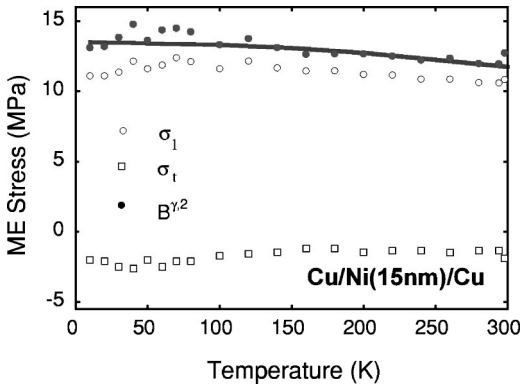

FIG. 4. Temperature dependence of the magnetoelastic stress $B_{eff}^{\gamma,2}$ for $t_{Ni}=15$ nm fitted using the form $B^{\gamma,2}(T)=B_{eff}^{\gamma,2}(0)m^2$ (continuous line).

forming lobules. For the 12 and 15 nm thick Ni films [Figs. 3(c) and 3(d)] the contrast is weaker and the domains size decreases down to about 0.5 μm. These results are in agreement with those reported by Bochi *et al.*[14] in similar Ni epitaxial films that show a transition in length scale of the domain size at $t_{Ni}=9.5$ nm.

IV. ANALYSIS

Figure 4 shows the temperature dependence of σ_l, σ_t, and $B_{eff}^{\gamma,2}$ for the 15 nm thick Ni film. The continuous line is a fit using the $B_{eff}^{\gamma,2}=B_{eff}^{\gamma,2}(0)m^2$ law, where m is the bulk reduced magnetization, $m=M(T)/M(0)$. Figure 5 displays the $B_{eff}^{\gamma,2}(0)$ values as a function of the internal in-plane strain $\epsilon_{\|}$.[3] The $B_{eff}^{\gamma,2}(0)$ values obtained for all the films studied are larger that the measured $B_{eff}^{\gamma,2}(0)$ for the 200 nm Ni film.[15] The experimental data show a trend for $B_{eff}^{\gamma,2}(0)$ to increase as the internal strain increases. The tentative fit $B+D\epsilon_{\perp}$ gives the values $B=10$ MPa, $D=250$ MPa, and is displayed in Fig. 5 (continuous line). It is clear that the B coefficient corresponds to the bulk value and that D can be associated to a strain contribution. The volume distortion in thin films and superlattices has been proposed to be a source of ME stress. As a result, the irreducible ME stress coefficient should have a contribution linear in the internal strain.

The facts found previously: the m^2 thermal dependence for $B_{eff}^{\gamma,2}(T)$ below room temperature, and the approximately linear relation between $B_{eff}^{\gamma,2}(0)$ and the internal strain, suggest that the ME stress in these Ni thin films is governed by volume effects. To interpret the empirical fits in Figs. 4 and 5, we use a phenomenological model that includes a strain-induced correction to the bulk ME constants.[16,17] The terms obtained from this contribution has been used to explain the anomalous behavior found in 3*d* thin films.[8,10] The ME energy density e_{ME} can be expressed to second-order in strains: $\Sigma_{ijmn}B_{ijmn}\epsilon_{ij}\alpha_m\alpha_n+\Sigma_{ijklmn}M_{ijklmn}\epsilon_{ij}\epsilon_{kl}\alpha_m\alpha_n$, $i,j=x,y,z$. B_{ijmn} and M_{ijklmn} are generalized first and second order ME coefficients, α_i's are direction cosines of the magnetization, and ϵ_{ij} components of the tensor strain. A similar approach was also taken by Ha *et al.* based on a spin-pair model.[18] For cubic symmetry, the ME contribution to the free energy density is written in terms of Cartesian strains, up to order $l=2$, and α_i's related to the Cartesian system fixed on the nickel axis [19] in such a way the x is lined with the cantilever beam direction ($[100]\|x,[010]\|y,[001]\|z$):

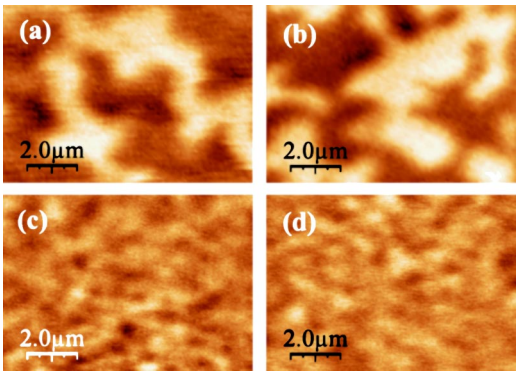

FIG. 3. Magnetic force microscope graphs performed on Cu/Ni/Cu films, (a) $t_{Ni}=6$ nm, (b) $t_{Ni}=8$ nm, (c) $t_{Ni}=12$ nm, (d) $t_{Ni}=15$ nm.

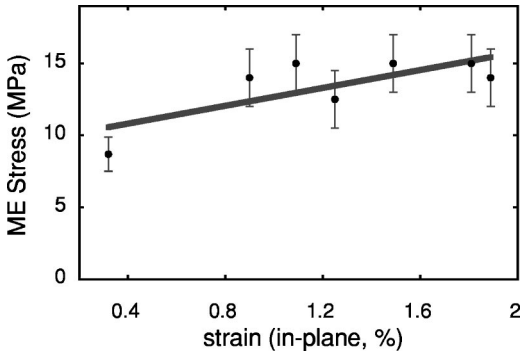

FIG. 5. Strain dependence of the magnetoelastic stress $B_{eff}^{\gamma,2}$ fitted using the form $B_{eff}^{\gamma,2}(0)=B^{\gamma,2}(0)+D^{\gamma,2}(0)\epsilon_{\|}$ (continuous line). For the Ni films, the data extrapolate at zero strain to $B^{\gamma,2}(0)=10$ MPa when $D^{\gamma,2}(0)=250$ MPa.

$$
\begin{aligned}
e_{\mathrm{ME}} = {} & B^{\gamma,2}\left[\left(\alpha_z^2-\frac{1}{3}\right)\left(\epsilon_{zz}-\frac{\epsilon_{xx}+\epsilon_{yy}}{2}\right)+\frac{1}{2}(\alpha_x^2-\alpha_y^2)(\epsilon_{xx}-\epsilon_{yy})\right] \\
& + M_1^{\gamma,2}\left[\left(\alpha_z^2-\frac{1}{3}\right)\left(\epsilon_{zz}^2-\frac{\epsilon_{xx}^2+\epsilon_{yy}^2}{2}\right)+\frac{1}{2}(\alpha_x^2-\alpha_y^2)(\epsilon_{xx}^2-\epsilon_{yy}^2)\right] \\
& + M_2^{\gamma,2}\left[\left(\alpha_z^2-\frac{1}{3}\right)\left(\epsilon_{xx}\epsilon_{yy}-\epsilon_{zz}\frac{\epsilon_{xx}+\epsilon_{yy}}{2}\right)-\frac{1}{2}(\alpha_x^2-\alpha_y^2)\epsilon_{zz}(\epsilon_{xx}-\epsilon_{yy})\right] \\
& + M_3^{\gamma,2}\left[\left(\alpha_z^2-\frac{1}{3}\right)\left(\epsilon_{xy}^2-\frac{\epsilon_{yz}^2+\epsilon_{zx}^2}{2}\right)+\frac{1}{2}(\alpha_x^2-\alpha_y^2)(\epsilon_{yz}^2-\epsilon_{zx}^2)\right] \\
& + 2B^{\epsilon,2}(\alpha_y\alpha_z\epsilon_{yz}+\text{cyclic}) + 2M_1^{\epsilon,2}(\alpha_y\alpha_z\epsilon_{xx}\epsilon_{yz}+\text{cyclic}) + 2M_2^{\epsilon,2}[\alpha_y\alpha_z(\epsilon_{yy}+\epsilon_{zz})\epsilon_{yz}+\text{cyclic}] \\
& + 2M_3^{\epsilon,2}(\alpha_y\alpha_z\epsilon_{zx}\epsilon_{xy}+\text{cyclic}). \qquad (2)
\end{aligned}
$$

Therefore, the number of independent first-order ME coefficients is reduced to two ($B^{\gamma,2}$ and $B^{\epsilon,2}$ correspond to the usual B_1 and B_2 ME coefficients [20]), and six second-order irreducible ME coefficients ($M_i^{\gamma,2}$ and $M_i^{\epsilon,2}$, $i=1, 2, 3$). From Eq. (2) it can be deduced that different magnetization process produces different lattice deformations that are governed by the same ME coefficient. For example, for the γ terms, it can be observed that inside each square bracket strain polynomials proportional to $\alpha_z^2-1/3$ correspond to a tetragonal distortion $(a,a,a)\rightarrow(c,a',a')$ as the perpendicular component of **M** changes, while the second strain terms, which are multiplied by $\alpha_x^2-\alpha_y^2$, describe the breaking of the in-plane symmetry $(a,a)\rightarrow(a',b')$ due to the presence of **M** in the film plane (tetragonal base plane). Second-order terms introduce the coupling between strain components of the strain tensor with each other. Therefore, these terms are needed to analyze the effect of the strain field on the ME stress. Thus, it is interesting to point out that the $M_1^{\gamma,2}$ coefficient represents the coupling of the diagonal strain components with themselves ($\epsilon_{ii}\epsilon_{ii}$, $i=x,y,z$) while $M_2^{\gamma,2}$ show the coupling between different diagonal components ($\epsilon_{ii}\epsilon_{jj}$, $i,j=x,y,z, i\neq j$) and $M_3^{\gamma,2}$ couples nondiagonal deformations with themselves ($\epsilon_{ij}\epsilon_{ij}$, $i,j=x,y,z, i\neq j$). Notice that all the γ terms produce a tetragonal distortion in the cubic lattice.

The strain state of the thin film is introduced by writing the strain components as sum of the epitaxial and the magnetostrictive strain. In the case of biaxial misfit strain, $\epsilon_{xx}\rightarrow\epsilon_{xx}+\epsilon_{\parallel}$, $\epsilon_{yy}\rightarrow\epsilon_{yy}+\epsilon_{\parallel}$, $\epsilon_{zz}\rightarrow\epsilon_{zz}+\epsilon_{\perp}$, where $\epsilon_{\parallel}$ and $\epsilon_{\perp}$ are, respectively, the in-plane and out-of-plane misfit strain. In the Cu/Ni/Cu/Si(001) system the biaxial strain is caused in the nickel layer by the epitaxial growth on copper.[3] These misfit strains can be very large, $\epsilon_{\parallel},\epsilon_{\perp}>10^{-2}$, compared to the magnetostrictive strains, $\lambda<10^{-4}$. Taking the terms linear in $\epsilon_{\parallel}$ and $\epsilon_{\perp}$ we have [21]

$$
\begin{aligned}
E_{\mathrm{ME}}^{t} = {} & \left(\alpha_z^2-\frac{1}{3}\right)\left[B_{\mathrm{eff}}^{rs}+B_{1,\mathrm{eff}}^{\alpha,2}(\epsilon_{zz}+\epsilon_{xx}+\epsilon_{yy})\right. \\
& \left. + B_{2,\mathrm{eff}}^{\alpha,2}\left(\epsilon_{zz}-\frac{\epsilon_{xx}+\epsilon_{yy}}{2}\right)\right]+\frac{1}{2}B_{\mathrm{eff}}^{\gamma,2}(\alpha_x^2-\alpha_y^2)(\epsilon_{xx}-\epsilon_{yy}) \\
& + 2B_{\mathrm{eff}}^{\delta,2}\alpha_x\alpha_y\epsilon_{xy}+2B_{\mathrm{eff}}^{\epsilon,2}(\alpha_y\alpha_z\epsilon_{yz}+\alpha_z\alpha_x\epsilon_{zx}), \qquad (3)
\end{aligned}
$$

where the ME coefficients are written in terms of the first and second-order ME coefficient:

$$B_{\mathrm{eff}}^{rs} = -(\epsilon_{\parallel}-\epsilon_{\perp})\left[B^{\gamma,2}+(\epsilon_{\parallel}+\epsilon_{\perp})M_1^{\gamma,2}-\epsilon_{\parallel}M_2^{\gamma,2}\right], \qquad (4a)$$

$$B_{1,\mathrm{eff}}^{\alpha,2} = -\frac{1}{3}(\epsilon_{\parallel}-\epsilon_{\perp})[2M_1^{\gamma,2}-M_2^{\gamma,2}], \qquad (4b)$$

$$B_{2,\mathrm{eff}}^{\alpha,2} = B^{\gamma,2}+\frac{2}{3}\left[(\epsilon_{\parallel}+2\epsilon_{\perp})M_1^{\gamma,2}+\left(\epsilon_{\parallel}+\frac{1}{2}\epsilon_{\perp}\right)M_2^{\gamma,2}\right], \qquad (4c)$$

$$B_{\mathrm{eff}}^{\gamma,2} = B^{\gamma,2}+2\epsilon_{\parallel}M_1^{\gamma,2}-\epsilon_{\perp}M_2^{\gamma,2} \equiv B^{\gamma,2}+\epsilon_{\parallel}D^{\gamma,2}, \qquad (4d)$$

$$B_{\mathrm{eff}}^{\delta,2} = B^{\epsilon,2}+\epsilon_{\perp}M_1^{\epsilon,2}+2\epsilon_{\parallel}M_2^{\epsilon,2}, \qquad (4e)$$

$$B_{\mathrm{eff}}^{\epsilon,2} = B^{\epsilon,2}+\epsilon_{\parallel}M_1^{\epsilon,2}+(\epsilon_{\parallel}+\epsilon_{\perp})M_2^{\epsilon,2}. \qquad (4f)$$

Equation (4d) corresponds to the strain contribution to the ME coefficient. The first term is the first-order ME coefficient, the term proportional to $M_1^{\gamma,2}$ is the change in the ME stress due to the isotropic variation of the in-plane lattice parameter, while the last term is due to the strain perpendicular to the *xy* plane in which the ME stress is measured. Now the equation lineal in the in-plane strain, used to fit the data in Fig. 5, is obtained from Eq. (4d) using $\epsilon_{\perp}=-(2c_{12}/c_{11})\epsilon_{\parallel}$ that is well followed by the films studied here.[3] Therefore, $B_{\mathrm{eff}}^{\gamma,2}=B^{\gamma,2}+\epsilon_{\parallel}D^{\gamma,2}$, with $D^{\gamma,2}=2[M_1^{\gamma,2}+(c_{12}/c_{11})M_2^{\gamma,2}]$. The thermal dependence of the ME stresses in 3*d* metals show, contrarily to the rare earth systems, large discrepancies with the standard Callen and Callen law:[22] $\hat{I}_{l+1/2}[\hat{m}]$, where $\hat{I}_{l+1/2}$ is the reduced hyperbolic Bessel functions, $\hat{m}=\mathcal{L}^{-1}[m(T)]$, and $\mathcal{L}^{-1}$ the inverse Langevin function. The reason appears to be the itinerant character of the magnetic moment.[23] Thus, in bulk nickel, $B^{\gamma,2}$ below 400 K follows a m^2 law and $B^{\delta,2}$ is fitted using a m^2+m^8 law.[24] Although a microscopic model for ME coupling in 3*d* metals is needed to explain such thermal dependence, we can discuss or consider the thermal dependence of $B_{\mathrm{eff}}^{\gamma,2}$ in the Cu/Ni/Cu films in terms of the symmetry of the phenomenological expression for e_{ME} [Eq. (2)] and the known thermal dependence of $B^{\gamma,2}$ and $B^{\delta,2}$ in terms of the reduced magnetization. By construction, the order *l* of the magnetization-polynomial representation is the

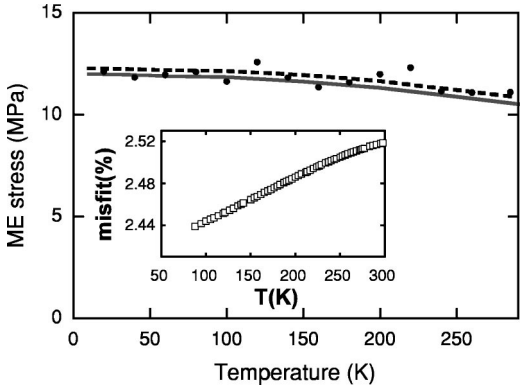

FIG. 6. Temperature dependence of the ME stress $B_{\text{eff}}^{\gamma,2}$ for $t_{\text{Ni}}=8$ nm fitted using the form $B^{\gamma,2}(T)=B_{\text{eff}}^{\gamma,2}(0)m^2$ (continuous line) and the expression $B_{\text{eff}}^{\gamma,2}(T)=[B^{\gamma,2}(0)+\epsilon(T)D^{\gamma,2}(0)]m^2(T)$, where $B^{\gamma,2}(0)=10$ GPa and $D^{\gamma,2}(0)=250$ GPa and the thermal dependence for the misfit strain shown in the inset (dashed line). The latter fit have been shifted to show that both fits allow one to obtain the same values for $D^{\gamma,2}(0)$.

same for the first and second-order ME terms. Thus, assuming that the thermal dependence is associated with the symmetry of the magnetization polynomials $B_{\text{eff}}^{i,2}(T)$ has to include terms proportional to m^2+m^8 and m^2. But looking now at the expression for $B_{\text{eff}}^{\gamma,2}$ we note that the M's coefficients, used to explain the strain dependence of $B_{\text{eff}}^{\gamma,2}(0)$, involves terms coming from the γ subspace, which can be identified by the $B^{\gamma,2}$ and $M_i^{\gamma,2}$, $i=1,2,3$, coefficients. If we extend our hypothesis about the origin of the m dependence of the B's and M's to reside in the symmetry of the representation from which they came, either γ or δ, we can conclude that $B_{\text{eff}}^{\gamma,2}(T)$, with terms from the γ representation, should go with the same law that $B^{\gamma,2}(T)$ which is m^2.

Since the epitaxial strains, $\epsilon_{\parallel}$ and $\epsilon_{\perp}$, are proportional to the misfit [3] η between the lattice parameters of copper a_{Cu} and nickel $a_{\text{Ni}}(\eta=a_{\text{Cu}}-a_{\text{Ni}}/a_{\text{Cu}})$ another source for additional thermal effects on the second-order contribution to the ME stress could be the temperature dependence of this misfit strain due to differential thermal expansion. The evaluation of $\eta(T)$ from $a_{\text{Cu}}(T)$ and $a_{\text{Ni}}(T)$ (Ref. 25) gives for $[\eta(80)-\eta(280)]/\eta(280)$ a value of about -3.8%, see the inset in Fig. 6. $\eta(T)$ increases with temperature while m^2 decreases from 0 to 280 K about a 10%. This fact implies that the second-order ME contribution ϵM has a weaker temperature dependence that the first-order one B.

Thus, including the temperature dependencies for the ME stress coefficients and the strain in Eq. (4d) we obtain that $B_{\text{eff}}^{\gamma,2}(T)=[B^{\gamma,2}(0)+\epsilon(T)D^{\gamma,2}(0)]m^2(T)$, where $m(T)$ is the reduced nickel bulk magnetization. Figure 6 shows, for the $t_{\text{Ni}}=8$ nm, the fit (dashed line) of $B_{\text{eff}}^{\gamma,2}(T)$ to the $B_{\text{eff}}^{\gamma,2}(T)=[B^{\gamma,2}(0)+\epsilon(T)D^{\gamma,2}(0)]m^2(T)$ expression where $B^{\gamma,2}(0)=10$ GPa and $D^{\gamma,2}(0)=250$ GPa are the values obtained from the analysis of the values of $B_{\text{eff}}^{\gamma,2}$ at 0 K vs $\epsilon_{\parallel}$. The thermal dependence for the misfit strain $\eta(T)$ is obtained from the thermal dependence of a_{Cu} and a_{Ni} from the data in Ref. 25. For comparison the fit using the $B_{\text{eff}}=B_{\text{eff}}(0)m^2$ law (continuous line) is also displayed in Fig. 6. It can be observed that the negligible difference between the two fits (in Fig. 6 the latter fit, for clarity, has been slightly displaced) is due to the weak correction that the strain contribution has in the total thermal dependence of $B_{\text{eff}}^{\gamma,2}$.

This thermal dependence of the ME stress $B_{\text{eff}}^{\gamma,2}(T)$ can explain the increasing of the saturation field observed in the ME stress isotherms as the temperature decreases from 290 K. Two main contributions to the effective magnetic anisotropy coefficient, namely, the magnetostatic term $2\pi M_s^2$ and the ME term $B_{\text{eff}}\epsilon(t)$, depend on the temperature as m^2: $-2\pi M_s^2+B_{\text{eff}}\epsilon(t)=[-2\pi M_s^2(0)+B_{\text{eff}}(0)\epsilon(t)]m^2$. The term in parenthesis has a weak thermal dependence while the stronger thermal dependence is in m^2, which decreases as temperature increases. Notice that the change in the saturation field is not due to the intrinsic magnetocrystalline anisotropy which is orders of magnitude smaller than the stress-induced anisotropy.

The cantilever deflection measurements due to transverse magnetization show a change in sign, from positive to negative values, as the t_{Ni} increases to values with effective in-plane anisotropy constant. A positive value of σ_t for $t_{\text{Ni}}=5$, 8 nm can be understood assuming a remnant state formed by domains with its magnetization vector along the out-of plane direction, as is suggested by the MFM images, Figs. 3(a) and 3(b). In this case the magnetization process consists in the rotation of **M** from the in-plane [100] direction to the [001] direction. It can be shown[15,24] that such magnetization process in the case of thin film results, for the transversal direction, in a magnetostrictive deformation with the same sing as that observed along the applied field direction. The negative, but small values of the 15 and 12 nm thick Ni films, indicates the decreasing volume of magnetic domains with magnetization pointing out of the perpendicular direction. The existence of canted structures due to the presence of competing second, $\propto\sin^2\theta$, and forth order, $\propto\sin^4\theta$ magnetic anisotropy [18] can explain the smaller contrast observed in the domain patterns [26] and the negative values of σ_t in the 12 and 15 nm thick films.

The study of the thermal dependence of ME stress in Cu/Ni/Cu thin films have revealed volumelike contributions due to the tetragonal distortion of the nickel blocks. This fact has been deduced from the thermal dependence of the irreducible ME stress and the thickness dependence of $B_{\text{eff}}^{\gamma,2}$ at 0 K. These effects have been explained by extending the cubic ME energy up to second-order in strain to include the effects due to the large internal strain found in the nickel layers. The thermal dependence of $B_{\text{eff}}^{\gamma,2}$ that has the same dependence that $B^{\gamma,2}$ for nickel bulk is explained in terms of the symmetry of the second-order ME contribution to the ME energy density.

ACKNOWLEDGMENTS

We acknowledge Spanish MCyT for financial support under Project No. MAT2000-1290-C03-01. The work done at MIT was supported by NSF Grant No. DMR-0105423. M.C. also thanks MCyT for financial support. Dr. J.K. Ha is acknowledged for discussions and preparation of the films. We also thanks J. A. Rodriguez for help in some experimental work.

*Electronic address: ciria@unizar.es; URL: www.unizar.es/ciria. Also at Department of Materials Science and Engineering, Massachusetts Institute of Technology, Cambridge, Massachusetts, USA.

[1] H. Ohno, Science **281**, 951 (1998).
[2] D. Sander, Rep. Prog. Phys. **62**, 809 (1999).
[3] K. Ha, M. Ciria, R. C. O'Handley, P. W. Stephens, and S. Pagola, Phys. Rev. B **60**, 13780 (1999).
[4] M. Bibes, S. Valencia, Ll. Balcells, B. Martínez, J. Fontcuberta, M. Wojcik, S. Nadolski, and E. Jedryka. Phys. Rev. B **66**, 134416 (2002).
[5] R. Naik, A. Poli, D. McKague, A. Lulaszew, and L. E. Wenger, Phys. Rev. B **51**, 3549 (1995).
[6] J. I. Arnaudas, M. Ciria, L. Benito, C. De la Fuente, M. R. Ibarra, A. del Moral, M. Bibes, Ll. Balcells, and J. Fontcuberta, J. Magn. Magn. Mater. **272–276**, 2100 (2004).
[7] M. Stampanoni, A. Vaterlaus, M. Aeschlimann, and F. Meier, Phys. Rev. Lett. **59**, 2483 (1987).
[8] G. Wedler, J. Walz, A. Greuer, and R. Koch, Phys. Rev. B **60**, R11313 (1999).
[9] Th. Gutjahr-Löser, D. Sander, and J. Kirschner, J. Magn. Magn. Mater. **220**, L1 (2000).
[10] Th. Gutjahr-Löser, D. Sander, and J. Kirschner, J. Appl. Phys. **87**, 5920 (2000).
[11] A. del Moral, M. Ciria, J. I. Arnaudas, M. R. Wells, R. C. C. Ward, and C. de la Fuente, J. Phys.: Condens. Matter **10**, L139 (1998).
[12] E. du Tremolet de Lacheisserie and J. C Peuzin, J. Magn. Magn. Mater. **136**, 189 (1994).
[13] H. J. McSkimin, J. Appl. Phys. **24**, 988 (1953).
[14] G. Bochi, H. J. Hug, D. I. Paul, B. Stiefel, A. Moser, I. Parashikov, H. J. Güntherodt, and R. C. O'Handley, Phys. Rev. Lett. **75**, 1839 (1995).
[15] M. Ciria, J. I. Arnaudas, L. Benito, C. de la Fuente, A. del Moral, J. K. Ha, and R. C. O'Handley, Phys. Rev. B **67**, 024429 (2002).
[16] R. C. O'Handley and S. W. Sun, J. Magn. Magn. Mater. **104–107**, 1717 (1992).
[17] S. W. Sun and R. C. O'Handley, Phys. Rev. Lett. **66**, 2798 (1991).
[18] K. Ha and R. C. O'Handley, J. Appl. Phys. **85**, 5282 (1992).
[19] J. Rouchy and E. de Lacheisserie, Z. Phys. B **36**, 67 (1979).
[20] R. C. O'Handley, *Modern Magnetic Materials: Principles and Applications* (Wiley, New York, 2000).
[21] M. Ciria and R. C. O'Handley, J. Magn. Magn. Mater. **240**, 464 (2002).
[22] E. R. Callen and H. B. Callen, Phys. Rev. **139**, A455 (1965).
[23] A. del Moral, *Magnetostriction: Basic Principles and Materials* (Institute of Physics, Bristol, 2004).
[24] Betz and E. du Tremolet de Lacheisserie, Appl. Phys. Lett. **68**, 132 (1996).
[25] F. C. Nix and D. MacNair, Phys. Rev. **60**, 597 (1941).
[26] P. J. A. van Schendel, Ph. Thesis, University of Basel, 2000.